Computational Materials Science 161 (2019) 99–106

Contents lists available at ScienceDirect

Computational Materials Science

journal homepage: www.elsevier.com/locate/commatsci

Successful test of the classical nucleation theory by molecular dynamic simulations of BaS

Sandra Cristina Costa Prado[a], José Pedro Rino[b,d,*], Edgar D. Zanotto[c,d]

[a] Faculdade de Tecnologia de Mococa, Ave. Dr. Américo Pereira Lima, s/n, 13736-260 Mococa, SP, Brazil
[b] Departamento de Física, Universidade Federal de São Carlos, Via Washington Luiz km. 235, 13565-905 São Carlos, SP, Brazil
[c] Departamento de Engenharia dos Materiais, Universidade Federal de São Carlos, Via Washington Luiz km. 235, 13565-905 São Carlos, SP, Brazil
[d] Center for Research, Technology and Education in Vitreous Materials, Universidade Federal de São Carlos, São Carlos, SP, Brazil

ARTICLE INFO

Keywords:
Nucleation
Crystal growth
Molecular dynamics simulation
Supercooled liquid region
Barium sulfide

ABSTRACT

We used a recently developed two-body interatomic potential for barium sulfide (BaS), and performed molecular dynamics (MD) simulations with 36,000 particles to determine the kinetics of spontaneous, homogeneous nucleation and growth of BaS crystals in the supercooled liquid. Isothermal-isobaric MD simulations were accomplished at three temperatures. The calculated pair correlation function, along with several snapshots, allowed us to quantify the nucleation times, their crystal growth rates, and the time evolution of overall crystallization. Nucleation was spontaneously achieved in the supercooled liquid state; therefore, we computed the average birth times of the critical nuclei (also known as average onset time of the first nucleus) from 15 samples at each temperature, from which we computed the steady-state nucleation rates, MD $J_{ss}(T)$. Then, we independently obtained by MD the diffusion coefficients, $D(T)$, the melting point, T_m, and the enthalpy of melting, ΔH_m. Thus, the MD J_{ss} could be compared with the predictions of the Classical Nucleation Theory (CNT) for homogeneous nucleation using only one fitting parameter, the nucleus/liquid interfacial free energy, σ. The calculated critical nucleus is made of only 2 to 3-unit cells, which is consistent with the critical size observed in the simulations, approximately 10–15 atoms. Using a constant (fitted value of) σ, and the D(T) and thermodynamic parameters from the simulations, we found that the MD pre-exponential factor has the same order of magnitude as the theoretical value predicted by the CNT. To the best of our knowledge, this agreement of the predictions of CNT and MD simulations has seldom been reported. Therefore, our results corroborate the validity of the CNT for simple supercooled liquids.

1. Introduction

Molecular dynamics (MD) simulation is an atomistic method based on using a particular (potential) model that can describe the system properties. By integrating the classical equations of motion of all particles of the system, the phase space trajectories can be obtained, and, in principle, its properties can be computed. With the advent of faster computers and sophisticated software, different properties of glassy materials have been increasingly simulated using different toy models [1–4], or phenomenological interatomic potentials, such as the Pedone [5], Stillinger-Weber [6] and Buckingham [7–9] potentials, to cite some of the most used.

The first challenge for correctly simulating any material is to find an interatomic model that can adequately describe the materiaĺs structure and properties. The second is to assure that the model potential can replicate some experimental data that have not been used to parameterize the model [10]. Finally, in this particular study, since the model is intended to witness crystal nucleation and growth, it also should also be able to describe the crystallization process of the supercooled liquid (SCL).

The simplest and most common strategy to study nucleation and growth in supercooled liquids is by the seeding method [11,12], which relies on introducing a crystallite of a given size in a supercooled liquid and then letting the system evolve over time. If the crystallite is smaller than the critical nucleus size at the studied temperature, it will dissolve; if it is larger than that threshold, it will grow. This type of simulation successfully corroborates the main concepts of the classical nucleation theory, CNT [11] and allows for the determination of the critical nucleus size and growth rates, but not the nucleation rates versus temperature.

Some previous MD works have been published on this particular topic. The first study comparing simulating crystal-nucleation times and

* Corresponding author at: Departamento de Física, Universidade Federal de São Carlos, Via Washington Luiz km. 235, 13565-905 São Carlos, SP, Brazil.
E-mail address: djpr@df.ufscar.br (J.P. Rino).

https://doi.org/10.1016/j.commatsci.2019.01.023
Received 16 August 2018; Received in revised form 9 January 2019; Accepted 15 January 2019

theoretical predictions was reported by Aga et al. using aluminum as a model. [13] More recently, molecular dynamics simulations were performed for metallic systems in which spontaneous nucleation and grain growth was observed without any extra inducing factor. For instance, in multi-million atom simulations, Shibuta et al. [14,15] reported on the nucleation and crystal growth for supercooled liquid Iron, whereas Mahata et al. [16] investigated the homogeneous homogeneous nucleation from the respective supercooled liquids, determined the nucleus birth times and then calculated the related nucleation rates as a function of temperature for these simple metallic systems.

Shibuta et al. [14,15] showed that the temperature dependence of the nucleation rates and nucleation times of supercooled Fe show the characteristic nose shape, which is an indication of thermally activated nucleation. They observed that the grain growth exponent deviated from the ideal value and attributed their results to the anisotropy in the grain boundary energy, mobility of the grain boundary and dimensionality of the simulation cell.

In a billion-atom simulation of supercooled liquid Fe, Shibuta et al. [17] suggested that a very unusual mechanism controls the crystallization process. The first nuclei that formed stochastically, homogeneously and independently, acted as "nucleation sites" for the next wave of nuclei, i.e., apparently the second and following nuclei formed preferentially and clustered around the first-born nuclei. The authors mention that "some satellite-like small grains surrounding previously formed large grains exist in the middle of the nucleation process, which are not distributed uniformly". To the best of our knowledge, this type of "mixed" nucleation mechanism was reported for the first and only time in [17].

Mahata et al. [16] showed that there is a difference between simulations carried out isothermally and during quenching. They demonstrated that the solidification process could be clearly divided into three regimes; sub-critical where nucleation is unstable, super-critical where nucleation is stable, and solid-state grain growth regime by well-known experimental observations. They did not compare the MD nucleation rates with the theoretical values. However, they compared the critical nucleus size determined by MD with the CNT predictions. Their CNT estimates of the critical size, r_c, were higher than the MD simulations, $r_{c\text{-}MD}$, for relatively low nucleation temperatures, but they become quite close above 650 K. A possible reason for this difference is that the authors assumed that the nucleus/liquid interfacial free energy, σ, is temperature independent in the CNT calculations. However, using a (more realistic) positive temperature dependent σ would result in a decrease in the critical size calculated by CNT at lower temperatures and a better agreement with the MD results. We make a similar comparison of the calculated R*(CNT) versus the R^*_{MD} in this article. The results will be discussed later on in this article.

Of special interest to this study is the work of Norman and Pisarev [4], where the nucleation rates of supercooled Al were computed by MD simulation and compared with the estimates of CNT. By using two fitting parameters: the kinetic factor and the interfacial free energy, these authors have shown that the nucleation frequencies obtained from their simulations were comparable with the estimates by CNT within 1 order of magnitude. However, it should be noted that the two most important properties were fitted, therefore this can hardly be considered a test of the theory.

In this article we also compute the nucleation rates and compare them with theoretical estimates. We study the spontaneous nucleation in a more complex system having two chemical species. Our objective is to shed light on the kinetics of nucleation and growth in the early stages of crystallization by using a very good available potential for BaS [18], recently developed by one of us. This potential describes the structure of this supercooled liquid and its isochemical crystal phases very well. It is relevant that this SCL undergoes (detectable) spontaneous homogeneous nucleation and that such atomic level details are extremely hard (practically impossible) to detect experimentally. Hence, MD simulations can be extremely useful for this type of study. Here we not only determine the nucleation rates and the critical nucleus sizes as a function of temperature, but we also compute the diffusion coefficients, and then analyze the nucleation rates in terms of the CNT using only one fitting parameter, the interfacial free energy.

BaS was chosen for this study because it is an important infrared transmitting chalcogenide, having only two atomic species of mixed ionic character with some degree of covalency. In addition, in preliminary simulation runs we have observed spontaneous crystallization in the supercooled regime within reasonable MD simulation time scales. Finally, the empirical model developed by one of us describes very well several structural and physical properties of the system [18]. Therefore, BaS seems to be a perfectly adequate model material to test nucleation theories.

In the following sections, we first describe the effective pair potential and the computational details of the simulations (Section 2), followed by the results and discussion (Section 3). Final remarks on both the approach and results are presented in Section 4.

2. The interatomic model and computational details

The effective pair potential recently proposed by Rino [18], for barium sulfide consists of 4 terms: steric repulsion, Coulomb interactions due to charge transfer between ions, charge-induced dipole attractions due to the electronic polarizability of anions, and van der Waals attraction. The mathematical expression for this potential is given by

$$\Phi(r) = \sum_{i<j=1}^{N} V_{ij}(r) \tag{1}$$

where

$$V_{ij}(r) = A\left(\frac{\sigma_i + \sigma_j}{r}\right)^{\eta_{ij}} + \frac{Z_i Z_j}{r}\cdot e^{-\frac{r}{\lambda}} - \left(\frac{\alpha_i Z_j^2 + \alpha_j Z_i^2}{2r^4}\right)\cdot e^{-\frac{r}{\xi}} - \frac{W_{ij}}{r^6} \tag{2}$$

Here, σ_k is the ionic radius of each atom, Z_k is the effective charge of the ions in units of electronic charge, α_k is the electronic polarizability, A is the intensity of the steric repulsion and W is the intensity of the van der Waals attraction. η, λ, and ξ stand for the exponents of the steric repulsion, the screening lengths for the Coulomb and charge-dipole interactions, respectively. The potential is truncated at $r = r_c$. For $r < r_c$ the potential is shifted to make it and its first derivative continuous at r_c [19,20].

We carried out the parameterization of the interatomic potential taking into account the cohesive energy and bulk modulus at the experimental density of the material. All the parameters used to validate this effective pair potential are given in Ref. [18]. Some properties that were not used in the potential parameterization, such as a structural phase transformation under hydrostatic pressure and the vibrational density of states, were then used for its successful validation, and are also discussed in Ref. [18].

Initially, a Face-Centered Cubic (FCC) BaS single crystal was generated with 36,000 particles (18,000 Ba and 18,000 S) in a box with dimensions $L_x = L_y = 191.68$ Å, and $L_z = 31.95$ Å at the experimental density of this substance. Such dimensions refer to a system comprising 30-unit cells in the x and y directions and 5-unit cells in the z-direction. This strategy helped to visualize and identify formations of the first nuclei.

We applied periodic boundary conditions in all directions and used the Verlet algorithm to integrate the equations of motions with a time step of 1.5 fs. The initial rock salt structure at 50 K was heated until 3400 K in ramps of 50 K every 10,000-time steps. At this high temperature, the liquid was allowed to thermalize for 50,000-time steps. It was then quenched using the same rate as that used to melt the system, down to the initial temperature. All simulations were done using the LAMMPS package [21] in an NPT ensemble. Fig. 1 displays the energy per particle as a function of temperature during the heating and cooling

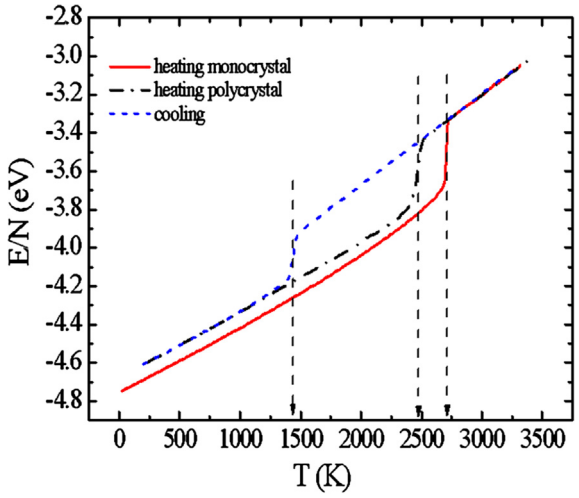

Fig. 1. Energy per particle as a function of temperature for the heating (single and polycrystal) and cooling procedures.

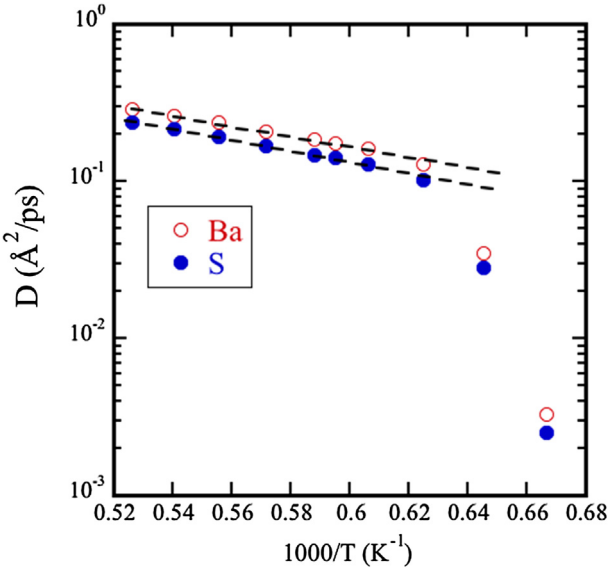

Fig. 2. Temperature dependence of the self-diffusion coefficients for Ba and S in the supercooled liquid state. The dashed lines show the respective Arrhenius fits. A breakdown takes place below 1650 K, where the supercooled liquid crystallizes directly on the cooling path.

procedures.

The final structure after cooling the liquid down to 50 K is a recrystallized polycrystalline rock salt material [18]. By repeating the heating procedure for the recrystallized phase, we observed that the mechanical melting temperature occurs at a lower temperature than that of the single crystal (Fig. 1). The melting curve shows a large hysteresis, with a wide supercooled region. We determined the melting temperature through the phase coexistence method, resulting in $T_m = 2450 \pm 20$ K [18].

Spontaneous nucleation was studied in the supercooled region. Starting from the equilibrium liquid above the (highest) melting point with a cooling rate of 0.83 K/ps, we investigated the time evolution of the system at 1900, 1800, 1750, 1700, 1650, 1600, 1550 and 1500 K. At 1750 K, 1700 K, and 1650 K, each system was allowed to evolve for 450 ps in the NPT ensemble. Above 1750 K, no nucleation event was observed in this time window. Below 1650 K, for the same cooling rate, nucleation already started on the cooling path. We used fifteen simulation samples at each temperature to obtain the statistical significance. The analyses of the atomic configurations and their visualization were performed using the OVITO (Open Visualization Tools) software [22] and the grain sizes for all snapshots were measured using the Fiji software [23].

3. Results and discussion

The main objective of this work was to detect the birth of the first nuclei and compute the spontaneous, homogeneous nucleation rates in the SCL state, then, to compare the obtained crystal nucleation rates with the predictions of the Classical Nucleation Theory (CNT). For that purpose, we needed the following parameters: diffusion coefficient, D (T), surface energy, σ, and the melting point, T_m, melting enthalpy, ΔH_m, and unit cell volume, V_c(T). In this work, we obtained all the above-listed parameters, except the interfacial energy, directly from the simulations, and then used two classical formulas to calculate a lower and an upper bound of the thermodynamic driving force per unit volume, ΔG_v(T). In the following sections, we describe how we obtained all these properties, analyze the nucleation rates, and compare them with theoretical estimates. Finally, we discuss the results.

3.1. Diffusivity

From the atomic mean square displacements, $\langle R^2(t)\rangle$ (not shown), we calculated the self-diffusion coefficients using the Einstein relation, $D = \frac{\langle R^2(t)\rangle}{6t}$ at nine temperatures in the SCL region. Fig. 2 displays the resulting *D(T)* as a function of temperature for Ba and S.

Diffusivity is (typically) a simple thermally activated process that can be fitted by an Arrhenius expression, $D = D_0 exp(-\frac{E_A}{k_B T})$, where E_A is the activation energy and D_0 a pre-exponential factor. For temperatures above 1650 K, the computed activation energies are: $E_A = 0.65 \pm 0.02$ eV for Ba and $E_A = 0.69 \pm 0.02$ eV for S, whereas the pre-exponential factors are 16 ± 2 Å^2/ps and 17 ± 2 Å^2/ps, respectively. Therefore, Ba is somewhat faster than S. For lower temperatures ($T < 1600$ K), the system crystallized on the cooling path, hence the diffusivity breakdown and becomes much smaller than predicted by the above equations, which is only valid for the supercooled liquid. The average of these values for Ba and S will be used to analyze crystal nucleation rates in terms of the CNT.

3.2. Crystal nucleation kinetics and analyses via CNT

We based the detection of the nucleation and crystal growth processes on analyses of snapshots of the atomistic configurations using OVITO. We used a common neighbor analysis (CNA [24–26]) routine to identify the local environments of the particles and compute the number of FCC structures forming as a function of time. We used the adaptative CNA procedure, where the cutoff is variable [25]. This action was necessary because another type of structural arrangement, hexagonal close-packed, however in smaller numbers, also emerged from our analysis of the crystallization process.

From the fifteen samples considered at 1750 K, only two displayed nucleation during the 450 ps simulation time. At 1700 K, eight samples underwent nucleation, and at 1650 K, all 15 samples nucleated. This is an indication of the stochastic process underlining nucleation. Immediately after the critical-sized nuclei were born, they underwent spontaneous grain growth. Fig. 3 shows a representative snapshot of the atomistic configuration for the three studied temperatures at five time periods. The FCC atoms are shown in green (only online version), and unknown structures in grey.

On average, nucleation happens earlier and more frequently at 1650 K than at higher temperatures. At 1650 K, approximately 100 ps after the quenching procedure, crystals start to nucleate and grow. For shorter times, we observed the emergence of several (sub-critical size) embryos, which form and dissolve, as predicted by the CNT (see the supplementary video). This behavior is shown in Fig. 4, which displays

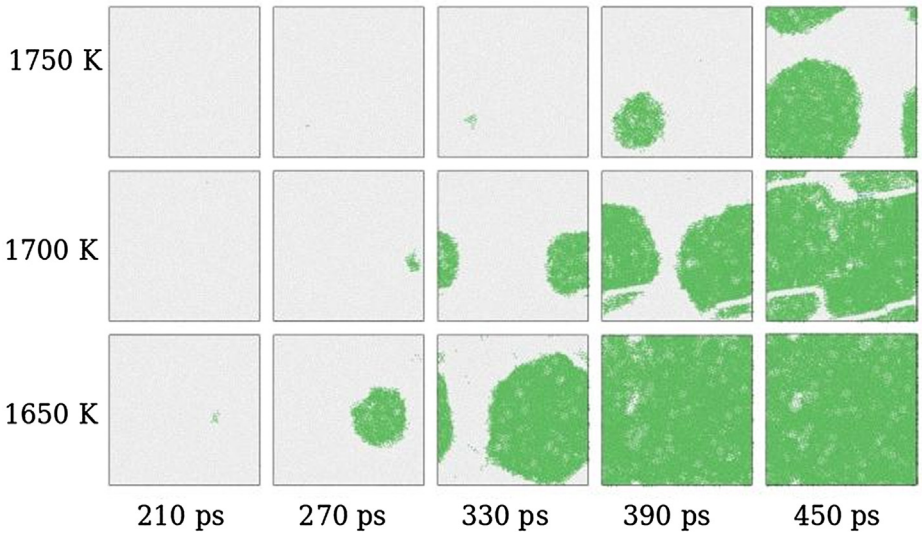

Fig. 3. Atomistic configuration as a function of time for three temperatures and five times. The CNA shows the beginning of crystal nucleation and growth. In this particular sample, we observe only one nucleus after 210 ps at 1650 K. A nucleus also appears after around 270 ps at 1700 K and 1750 K.

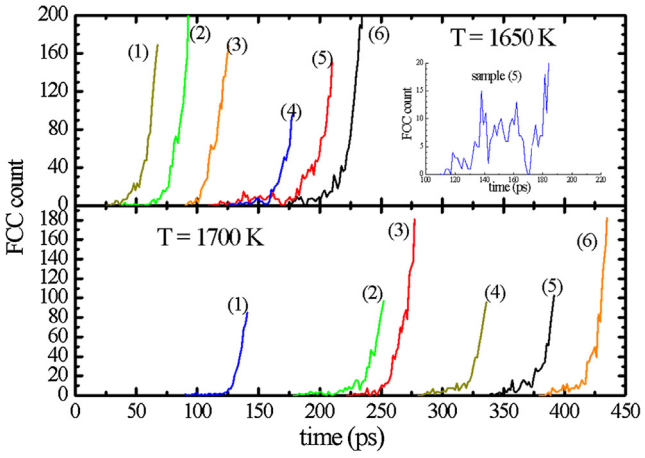

Fig. 4. Number of FCC atoms as a function of time for the first critical nucleus at 1650 K and 1700 K. Each line corresponds to a specific sample. The inset shows amplification of the birth of the first nucleus of sample 5.

the number of FCC atoms as a function of time including the birth of the first critical nucleus. The inset amplifies the beginning of the birth of a critical nucleus for sample number 5. The nucleus appears and dissolves a few times before reaching the critical size, which then undergoes continuous growth after 171 ps.

We used CNA analyses to determine the size of the first critical crystal nuclei and their birth time, for every sample. From these curves, the average time of birth at each temperature was computed. CNA calculations performed with OVITO also allowed us to determine the time evolution of the number of atoms in a nucleus (the growth rate). Table 1 summarizes the average birth time at 1650, 1680 and 1700 K. At 1750 K, statistics were not enough (only two nucleation events were detected) to compute these values.

Table 1
Average birth time of 15 samples each, as a function of temperature.

Temperature (K)	Average birth time (ps)
1650	122 ± 49
1680	170 ± 55
1700	266 ± 68

At each temperature, atoms start to agglutinate to minimize the overall energy of the system. Small fluctuations form and dissolve, whereas others – of critical size – nucleate and grow. At the three studied temperatures, we observed that the average, and even the shortest birth times are much larger than the average structural relaxation time, which means that the SCL relaxes well before nucleation begins. These results of the relaxation versus characteristic nucleation times will be extended to other temperatures and fully discussed in a forthcoming article.

Once the average onset time of the first nucleus, τ, is determined, the steady-state nucleation rate, J_{ss}, can be computed using the expression $J_{ss}(T) = \frac{1}{(V\tau)^{-1}}$, where V is the volume of the system (the simulation box size). In this case, it is implicitly assumed that steady-state nucleation conditions have been reached, which is a reasonable assumption for this particular case, because we are studying temperatures above that of the nucleation rate maximum. Extensive experiments on different supercooled glass-forming liquids demonstrated that non-stationary nucleation is significant and typical for temperatures at and below the temperatures of maximum nucleation rate [27,28]. Fig. 5 shows the resulting steady-state nucleation rates.

It is interesting to point out that the spontaneous nucleation rates calculated by MD for monoatomic metals lie in the range of 10^{30} to 10^{40} (m^{-3} s^{-1}) [4,15,16], whereas experimentally determined nucleation rates (for more complex, multicomponent systems) span a range from 10^{4} to 10^{20} (m^{-3} s^{-1}) [27].

Besides the birth times and diffusivity, the phase space trajectory obtained from MD simulation allowed us to obtain the crystal volume, V(T), melting point, T_m, and the enthalpy as a function of temperature and, consequently, the melting enthalpy, ΔH_m. With those values, the thermodynamic driving force, $\Delta G_v(T)$, could be calculated using the Turnbull definition for an upper bound, $\Delta G_v(T) = \frac{\Delta Hm}{V(T)}\frac{(T_m - T)}{T_m}$, or the Hoffman approximation for a lower bound: $\Delta G_v(T) = \frac{\Delta Hm}{V(T)}\frac{T(T_m - T)}{T_m^2}$. The real value lies somewhere between these two limits.

With all these parameters, we can now use the classical nucleation equation to analyze our MD data. According to that theory, the nucleation rate is given by [29]

$$J_{ss}(T) = \sqrt{\frac{\sigma}{k_B T}}\frac{D(T)}{d_0^4}\cdot exp\left[-\frac{16\pi\sigma^3}{3k_B}\cdot\frac{1}{T\Delta Gv^2}\right] \quad (6)$$

where k_B is the Boltzmann constant, $D(T)$ the diffusivity, d_0 the effective size of the diffusing units (or jump distance), which is expected to be of

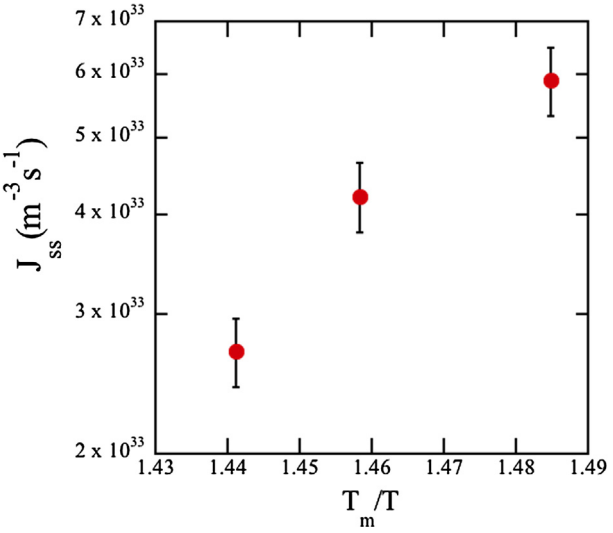

Fig. 5. Calculated steady-state nucleation rates as a function of inverse temperature, T. T_m is the melting point. The maximum nucleation rates could not be reached in our simulations due to copious crystallization of the samples on the cooling path for lower temperatures.

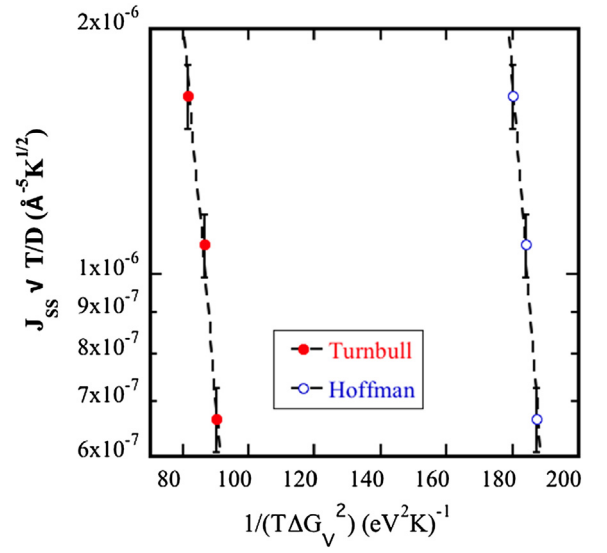

Fig. 6. $J_{ss}\sqrt{T}/D$ (in logarithmic scale) as a function of $1/(T.\Delta G_v^2)$ using the Turnbull and Hoffman equations for ΔG_v. The dashed lines show the fits using the classical nucleation equation.

Table 2
Estimated critical nucleus sizes and the interfacial free energies.

Temperature (K)	Critical nucleus size (Å)	σ (J/m²) Turnbull	σ (J/m²) Hoffman
1650	5.9	0.129	0.087
1680	6.2	0.130	0.089
1700	6.5	0.133	0.092
CNT fitting	–	0.131	0.139

the same order as the unit cell of the crystal phase. $\Delta G_v$is the driving force per unit volume of the crystal, and σ is the (unknown) nucleus/liquid interfacial free energy [27].

Fig. 6 shows the dependence of $J_{ss}\sqrt{T}/D$ as a function of $1/(T.\Delta G_v^2)$.

By fitting equation (6) to these data points, we can estimate the interfacial free energy (from the slope) and the pre-factor (from the intercept) as $\sigma = 0.131\ J/m^2$ and $J_0 = 9.4 \times 10^{47}\ K^{1/2}\,m^{-5}$ for the

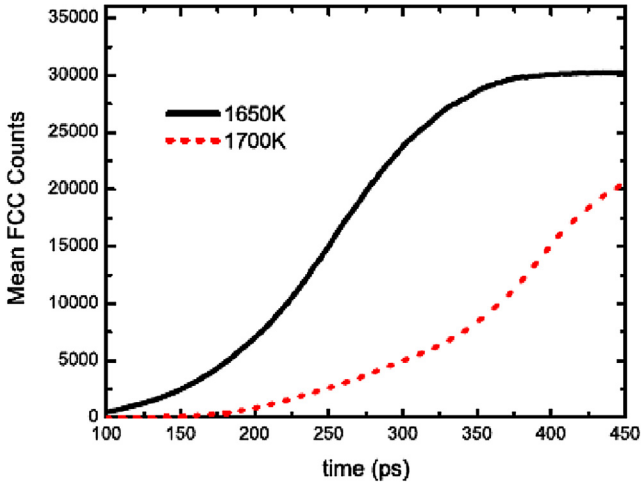

Fig. 7. Average number of FCC atoms (overall crystallization) as a function of time for two temperatures.

Turnbull model of ΔG_v, and $\sigma = 0.139\ J/m^2$ and $J_0 = 8.9 \times 10^{53}\ K^{1/2}\,m^{-5}$ for the Hoffman model.

The resulting average value of interfacial energy for BaS (0.131–0.139 J/m^2) are of same order of magnitude observed for typical values reported from the analysis of homogeneous nucleation in oxide glasses ($0.10 < \sigma < 0.25\ J/m^2$) [27], and a metallic system $\sigma \sim 0.17\ J/m^2$ [16]. By means of the phase trajectories resulting from the simulations, we can also obtain the number of FCC atoms and then estimate the critical nucleus radius (assuming spherical nuclei). In this way, using the calculated ΔGs and the relation $r_c = 2\sigma/\Delta G_v$, the interfacial free energy is obtained. The values at three temperatures are resumed in Table 2 showing that the σ calculated in two different ways, especially those obtained using the Turnbull equation for ΔG, are very similar. This fact reinforces the consistency of our procedures.

As the CNT predicts the "spherical" critical nucleus size as $r_c = 2\sigma/\Delta G_v$, we can calculate the size of the critical crystal as $l = \sqrt{4\pi/3}\,r_c$. Assuming that the diffusing units have approximately the average critical crystal size l, the theoretical values of the pre-exponential factor $J_{0\text{-theor}} = \sqrt{(\sigma/k_B)}.1/d_0^4$ are $J_{0\text{-theor}} = 5.9 \times 10^{47}\ K^{1/2}/m^5$ and $J_{0\text{-theor}} = 6.0 \times 10^{47}\ K^{1/2}/m^5$ considering the interfacial energy calculated by the Turnbull and Hoffman fittings, respectively. Therefore, the extrapolated value of the pre-exponential, calculated using the Turnbull approach for ΔG, is of the same order of magnitude as the values predicted by CNT! Even the Hoffman approximation yields a pre-exponential that is "only" 6 orders of magnitude larger than $J_{0\text{-theor}}$.

This is a very positive, yet surprising, result because previous analyses of experimental homogeneous nucleation in several oxide glass-formers, with the same procedure, using a (fitted) constant interfacial energy, always yield a pre-exponential term ($10^{60} < J_0\text{-exp} < 10^{90}\ K^{1/2}/m^5$) that is many orders of magnitude larger than the theoretical value ($10^{48}\ K^{1/2}/m^5$) [27]. However, it should be stressed that in all those previous analyses of experimental nucleation rates, in addition to using a constant (fitted) interfacial energy, an extra assumption was made about the diffusion coefficient, D(T). In the case of complex, multicomponent materials, D(T) is indefinite, hence researchers make use of the well-known Stokes-Einstein-Eyring (SEE) equation [$D(T) = k_BT/(d_0.\eta(T))$] and calculate D(T) using experimental viscosity, η(T), data. An alternative method is also used to infer D(T), when non-stationary nucleation rates are available (typically for temperatures at and below the temperature of the maximum nucleation rate, T_{max}). In this case, a few researchers have used the nucleation induction times, $t_{ind}(T)$, which should be related to the diffusivity. Both strategies lead to the above-described enormous discrepancy in the pre-exponential term [24]. In this work, however, we used the D(T) obtained directly from

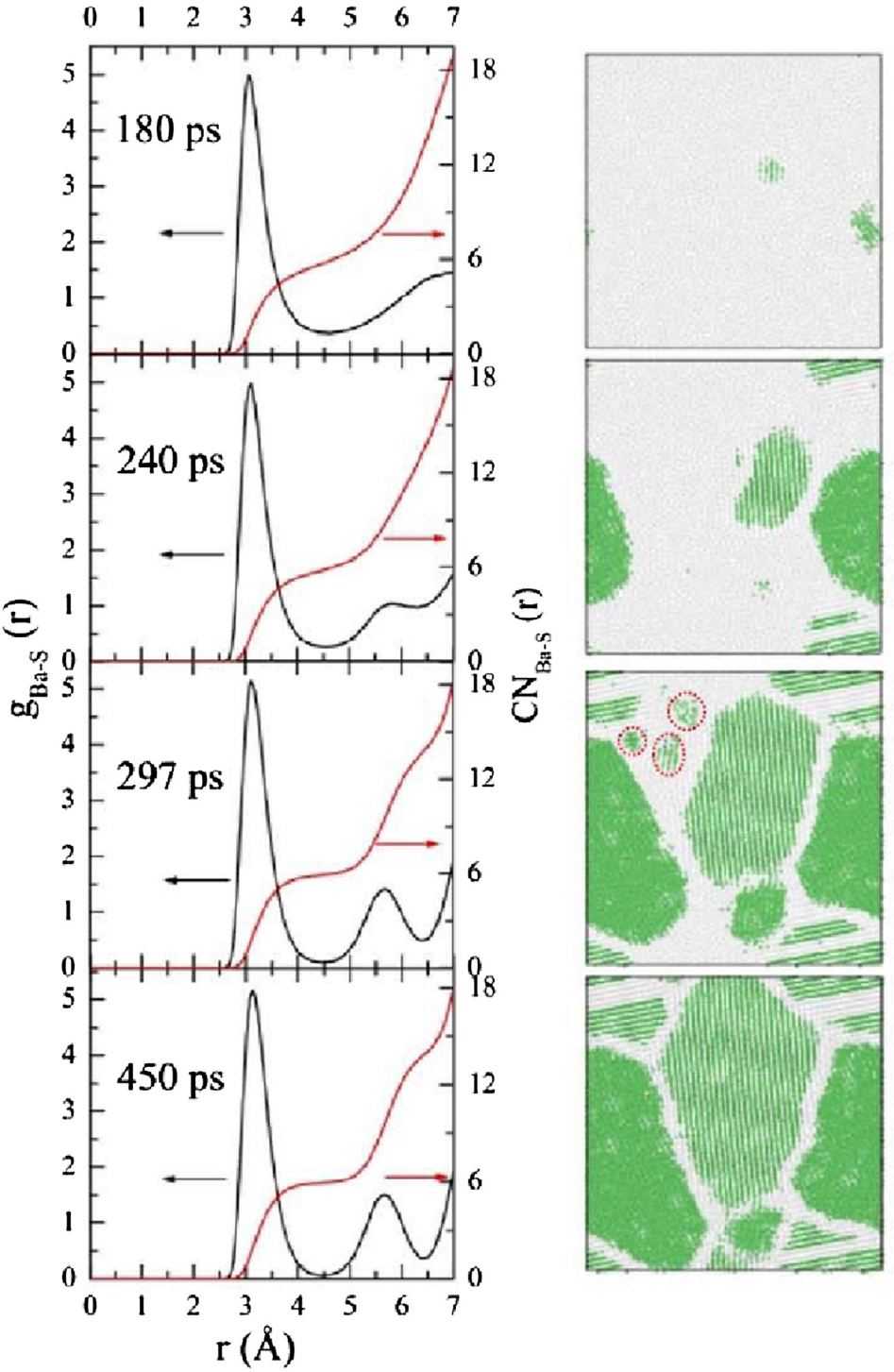

Fig. 8. Time evolution of the pair distribution function (left side) and the coordination number (right side) for a particular sample at 1650 K. The red circles highlight grains that dissolved or were aggregated to a bigger crystal.

the simulations, which is a key difference from the above-listed analyses of experimental studies, and provides one logical reason to explain why these previous experimental studies have not found such an agreement between measurements and calculations by CNT.

In a LJ model simulation [1] study, the authors have used the Turnbull approximation for ΔG, compared the pre-exponential with the theoretical factor and found a difference of about 6 orders of magnitude. In another example, the temperature dependence of the nucleation rate simulated by MD for supercooled Al [4] could by approximated by the CNT by fitting two parameters. The authors found that the kinetic factor and the critical nucleus size calculated by CNT are only 1.5–2.0 and 1.5–10 times larger, respectively, than the values obtained by their MD simulations. In summary, in this work, we observed that using only one fitting parameter (interfacial energy, which is very close to the value calculated from the critical nucleus size), and the Turnbull formula for ΔG, our MD simulations described the homogeneous nucleation kinetics in supercooled barium sulfide in an impressive agreement with the predictions of CNT.

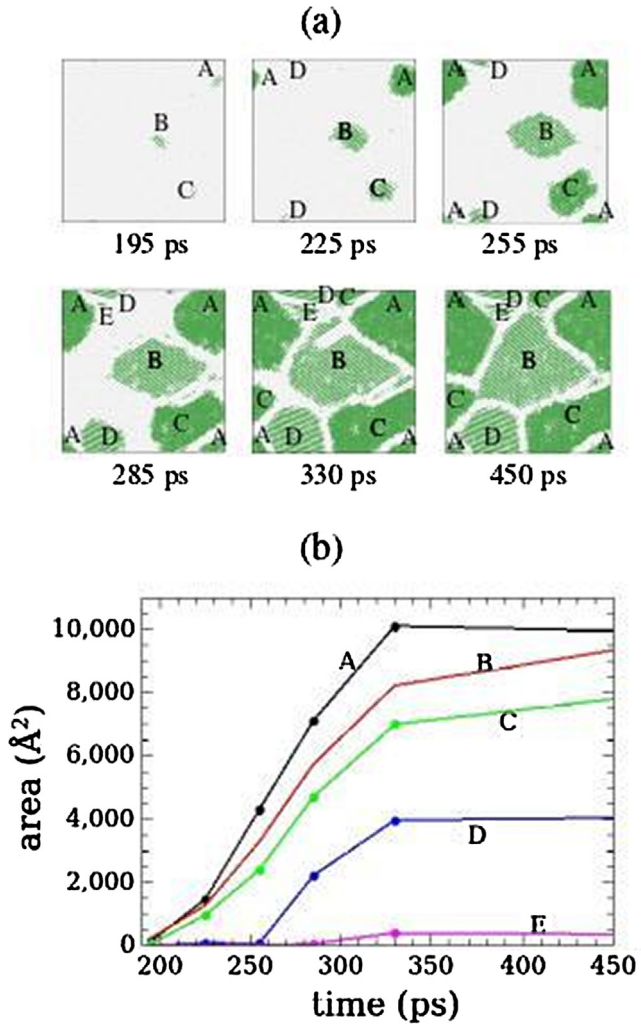

Fig. 9. (a) Representative snapshots of the atomistic configuration at 1650 K showing the beginning of nucleation and grain growth as a function of time. (b) The evolution of the area of each grain as a function of time.

3.3. Critical nucleus size

Another test of the predicting power of the CNT can be made by comparing the calculated and measured critical nucleus sizes. Using the interfacial energy and thermodynamic driving force, and assuming that the classical nucleation theory is valid, we can estimate the critical (spherical) nucleus size by $r_c = 2\frac{\sigma}{|\Delta G_v|}$. The volume of a critical nucleus is then $\mathrm{Vol_c} = \frac{4\pi}{3} r_c^3 = l^3$.

This estimate results in the size of the critical structure being in the range of 9 Å $\leq l \leq$ 11 Å and 15 Å $\leq l \leq$ 16 Å for Turnbull and Hoffman models of ΔG, respectively. Recalling that the unit cell parameter of the FCC barium sulfide is 6.387 Å, the critical nucleus to start the nucleation process consists of only a few unit cells. These values obtained from the CNT are consistent with the direct MD results shown in Fig. 4, i.e. approximately 6–8 atoms must be assembled in a critical nucleus before crystal growth takes over at 1650–1700 K. Table 2 above summarizes the estimated nucleus size as a function of temperature.

This result corroborates the ability of the CNT in describing the nucleation process in BaS. This is indeed a very positive result, but other tests with other materials would be advisable to confirm or not the current findings. However, a more sophisticated approach will be needed to obtain the interfacial energy directly from MD; then a definitive test of the validity of CNT, without any free parameter could be made.

3.4. Preliminary results of overall crystallization

To complete the analysis of phase transformation in this system, we also computed the isothermal evolution of the overall crystallization. Fig. 7 displays the average FCC counts as a function of time over all samples for two temperatures. An increasing number of FCC atoms appears over time. It is noticeable that, at 1650 K, the system is completely crystallized after 400 ps (all the 15 samples crystallized).

Fig. 8 shows the atomic configuration for a particular sample at selected instants and the corresponding pair-correlation function. The coordination numbers were also calculated. FCC (green) grains nucleate and grow as time goes by. The full width at half maxima of the first peaks in the g(r) function narrows down and a second peak around 5.5 Å appears. The corresponding coordination numbers (i.e., the area under the first peak in the g(r)) become very well-defined, resulting in a coordination number 6, which is typical of a rock salt crystal.

3.5. Preliminary observations of crystal growth

Fig. 9a shows a representative atomistic evolution of one sample at 1650 K, whereas the grain size as a function of time is depicted in Fig. 9b. After 450 ps, the system was completely crystallized. Some grains nucleated very late (see grain E) and could not grow because the previous grains blocked them. The crystal growth rate was then higher for the first (A, B and C).

Assuming a circular shape (although this is not perfectly true), an average radius defined as $R_{eff} = \sqrt{\frac{A}{\pi}}$ can be calculated. In the first 100 ps after each critical nucleus appears, the growth rate is similar for all grains (v_A= 0.462 Å/ps, v_B = 0.382 Å/ps, v_C = 0.379 Å/ps). However, as two or more grains impinge, their speed obviously decreases. Grain D appears only after 200 ps; later on, after 250 ps, it shows a continuous growth, with v_D= 0.400 Å/ps. For the considered sample, only grains B and C kept growing during the simulation time, while grains A and D stabilized after 330 ps. Grain E, instead, was entirely dissolved. Some coarsening was also observed (see grain B and its nearby region). These preliminary results are just to demonstrate that our simulations are adequate to follow crystal growth kinetics. Detailed studies of crystal growth will be continued and fully discussed in a forthcoming article.

4. Summary and conclusions

The pair potential used here for barium sulfide was quite adequate for describing several dynamical properties of this substance. For instance, the calculated pair correlation function, along with several snapshots, allowed us to quantify the evolution of the crystal nucleation and growth rates, and overall crystallization. Homogeneous nucleation occurred spontaneously in the SCL after quenching from the liquid state. From the average birth times, we computed the steady-state nucleation rates, MD $J_{ss}(T)$, at three temperatures in the supercooled liquid in the range 0.78–0.82 T_m. From the MD simulations we also obtained the diffusion coefficient, D(T), melting point, T_m, crystal volume, V(T), and the enthalpy of melting, ΔH_m. Using only one fitting parameter, the interfacial energy, the calculated (by CNT) critical nucleus sizes consist of only 2 to 3-unit cells, depending on the temperature and expression used for ΔG, and are consistent with the critical sizes observed in the birth time plots, i.e., approximately 10–15 atoms are needed to form a critical nucleus at these temperatures. This agreement suggests the validity of CNT.

The most relevant result of this work is that the magnitudes of the nucleation rates obtained by MD agree with the values predicted by the CNT. This test was made by using the D(T) and thermodynamic properties from the simulation, the Turnbull expression for ΔG, and an average (fitted value of) interfacial energy, σ. However, the resulting value of σ is close to an estimate made from the critical nucleus sizes obtained directly by MD. To the best of our knowledge, this positive test

of CNT from MD simulations for a binary material is quite original. This analysis reinforces the validity of the CNT, which, however, warrant further tests with other materials to validate and generalize the current findings.

CRediT authorship contribution statement

Sandra Cristina Costa Prado: Conceptualization, Formal analysis, Supervision, Validation, Visualization. **José Pedro Rino:** Conceptualization, Conceptualization, Formal analysis, Supervision, Validation, Visualization. **Edgar D. Zanotto:** Conceptualization, Formal analysis, Supervision, Validation, Visualization.

Acknowledgments

We would like to thank the São Paulo Research Foundation, FAPESP, Brazil (contract CEPID #2013/07793-6) and the National Council for Scientific and Technological Development, CNPq, Brazil (grant #301126/2015-1) for the financial support of this research.

Appendix A. Supplementary material

Supplementary data to this article can be found online at https://doi.org/10.1016/j.commatsci.2019.01.023.

References

[1] V.G. Baidakov, A.O. Tipeev, Crystal nucleation and the solid-liquid interfacial free energy, J. Chem. Phys. 136 (2012) 074510.
[2] M. Dzugutov, U. Dahlborg, Molecular-dynamics study of the coherent density correlation-function in a supercooled simple one-component liquid, J. Non-Cryst. Solids 131 (1991) 62–65.
[3] W. Kob, Computer simulations of supercooled liquids and glasses, J. Phys. – Condens. Matter 11 (1999) R85–R115.
[4] G.E. Norman, V.V. Pisarev, Molecular dynamics analysis of the crystallization of an overcooled aluminum melt, Russ. J. Phys. Chem. A+ 86 (2012) 1447–1452.
[5] A. Pedone, G. Malavasi, M.C. Menziani, A.N. Cormack, U. Segre, A new self-consistent empirical interatomic potential model for oxides, silicates, and silica-based glasses, J. Phys. Chem. B 110 (2006) 11780–11795.
[6] F.H. Stillinger, T.A. Weber, Computer-simulation of local order in condensed phases of silicon, Phys. Rev. B 31 (1985) 5262–5271.
[7] J. Du, A.N. Cormack, The medium range structure of sodium silicate glasses: a molecular dynamics simulation, J. Non-Cryst. Solids 349 (2004) 66–79.
[8] M.A.P. Silva, Y. Messaddeq, V. Briois, M. Poulain, F. Villain, S.J.L. Ribeiro, Structural studies on lead-cadmium fluoride solid solutions, Solid State Ionics 147 (2002) 135–139.
[9] M.A.P. Silva, A. Monteil, Y. Messaddeq, S.J.L. Ribeiro, Molecular dynamics simulations on devitrification: the PbF2 case, J. Chem. Phys. 117 (2002) 5366–5372.
[10] D.W. Brenner, The art and science of an analytic potential, Phys. Status Solidi B – Basic Res. 217 (2000) 23–40.
[11] J.K. Bording, J. Tafto, Molecular-dynamics simulation of growth of nanocrystals in an amorphous matrix, Phys. Rev. B 62 (2000) 8098–8103.
[12] J.R. Espinosa, C. Vega, C. Valeriani, E. Sanz, Seeding approach to crystal nucleation, J. Chem. Phys. 144 (2016) 034501.
[13] R.S. Aga, J.R. Morris, J.J. Hoyt, M. Mendelev, Quantitative parameter-free prediction of simulated crystal-nucleation times, Phys. Rev. Lett. 96 (2006).
[14] S. Okita, W. Verestek, S. Sakane, T. Takaki, M. Ohno, Y. Shibuta, Molecular dynamics simulations investigating consecutive nucleation, solidification and grain growth in a twelve-million-atom Fe-system, J. Cryst. Growth 474 (2017) 140–145.
[15] Y. Shibuta, K. Oguchi, T. Takaki, M. Ohno, Homogeneous nucleation and microstructure evolution in million-atom molecular dynamics simulation, Sci. Rep. – UK 5 (2015) 13534.
[16] A. Mahata, M.A. Zaeem, M.I. Baskes, Understanding homogeneous nucleation in solidification of aluminum by molecular dynamics simulations, Model. Simul. Mater. Sc. 26 (2018) 025007.
[17] Y. Shibuta, S. Sakane, E. Miyoshi, S. Okita, T. Takaki, M. Ohno, Heterogeneity in homogeneous nucleation from billion-atom molecular dynamics simulation of solidification of pure metal, Nat. Commun. 8 (2017).
[18] J.P. Rino, An interaction potential for barium sulfide: a molecular dynamics study, Comput. Mater. Sci. 92 (2014) 334–342.
[19] M.P. Allen, D.J. Tildesley, Computer Simulation of Liquids, Oxford University Press, Oxford, 1987.
[20] A. Nakano, R.K. Kalia, P. Vashishta, 1st sharp diffraction peak and intermediate-range order in amorphous silica – finite-size effects in molecular-dynamics simulations, J. Non-Cryst. Solids 171 (1994) 157–163.
[21] S. Plinton, Fast parallel algorithms for short-range molecular dynamics, J. Comput. Phys. 117 (1995) 1–19.
[22] A. Stukowski, Visualization and analysis of atomistic simulation data with OVITO-the open visualization tool, Model. Simul. Mater. Sci. Eng. 18 (2010) 015012.
[23] J. Schindelin, I. Arganda-Carreras, E. Frise, V. Kaynig, M. Longair, T. Pietzsch, S. Preibisch, C. Rueden, S. Saalfeld, B. Schmid, J.Y. Tinevez, D.J. White, V. Hartenstein, K. Eliceiri, P. Tomancak, A. Cardona, Fiji: an open-source platform for biological-image analysis, Nat. Methods 9 (2012) 676–682.
[24] J.D. Honeycutt, H.C. Andersen, Molecular-dynamics study of melting and freezing of small lennard-jones clusters, J. Phys. Chem. – US 91 (1987) 4950–4963.
[25] A. Stukowski, Structure identification methods for atomistic simulations of crystalline materials, Model Simul. Mater. Sc. 20 (2012).
[26] H. Tsuzuki, P.S. Branicio, J.P. Rino, Structural characterization of deformed crystals by analysis of common atomic neighborhood, Comput. Phys. Commun. 177 (2007) 518–523.
[27] V.M. Fokin, E.D. Zanotto, N.S. Yuritsyn, J.W.P. Schmelzer, Homogeneous crystal nucleation in silicate glasses: a 40 years perspective, J. Non-Cryst. Solids 352 (2006) 2681–2714.
[28] P.K. Gupta, D.R. Cassar, E.D. Zanotto, Role of dynamic heterogeneities in crystal nucleation kinetics in an oxide supercooled liquid, J. Chem. Phys. 145 (2016).
[29] J.W.P. Schmelzer, V.M. Fokin, A.S. Abyzov, Crystallization of glass: what we know, what we need to know, Int. J. Appl. Glass Sci. 7 (2016) 253–261.